IJCRT.ORG ISSN : 2320-2882

INTERNATIONAL JOURNAL OF CREATIVE RESEARCH THOUGHTS (IJCRT)

An International Open Access, Peer-reviewed, Refereed Journal

Synthesis and photoluminescence investigations on Sm^{3+} ions doped sodium alumino-borate phosphor

R. S. Palaspagar[1a], S. R. Khandekar[2]

[1]Department of Physics, Shivramji Moghe Mahavidyalay, Kelapur (Pkd) Dist. Yavatmal- 445001(M.S.), INDIA.

[2]Department of Chemistry, Indira Mahavidyalay, Kalamb, Dist. Yavatmal - 445401(M.S.), INDIA.

ABSTRACT

In the present work we describes mainly the optical absorption, photoluminescence (PL) characteristics of Sm^{3+} ions doped sodium alumino-borate phosphors $Na_2Al_2B_2O_7$ (NABO). The fine polycrystalline powder samples of NABO:Sm^{3+} has been prepared by a solution combustion technique. Powder X-ray diffraction and scanning electron microscopy studies were used to characterize the prepared combustion powder. Photoluminescence spectra revealed that samarium ions are present in trivalent oxidation states. The PL excitation spectra of NABO:Sm^{3+} consists of several bands peaking at 305 nm, 330 nm, 344 nm, 361 nm, 374 nm, 403 nm, 462 nm and 473 nm. The excitation spectrum monitored at 403 nm emission consists of green emission band peaking at 565 nm, orange emission band peaking at 603 nm and red emission band peaking at 651 nm. Since the prominent excitation peaks are above 350 nm, the phosphor may useful for solid state lighting application.

Keywords: Alumino-Borates, Combustion Synthesis, XRD, Photoluminescence, LED.

1. INTRODUCTION

Solid state inorganic borates have become a focus of technological interest due to a variety of physical and chemical properties. Inorganic Borates intrinsically possess characteristics that are advantageous for optical materials which include wide transparency range, large electronic band gap, good thermal and chemical stability, low preparative temperature, optical stability with good nonlinear characteristics and exceptionally high optical damage threshold. Several mixed metal borates (alumino-borates) are promising host materials for various dopant (activators and sensitizers) due to its stability [1]. Generally, RE doped glasses are better than the crystalline materials because of their broad inhomogeneous bandwidths, cheap production cost, good thermal stability, simple manufacturing process and high doping capability [2-7].

Among the RE ions Sm^{3+} ions display reddish orange emission in the visible region and having applications in the undersea communication, high density optical storage, color displays and visible solid-state lasers [8]. Further, Sm^{3+} ions doped glasses exhibit peculiar optical properties due to its 4G5/2 → 6HJ (J = 5/2, 7/2, 9/2 and 11/2) transitions in all host matrices. The spectroscopic study of Sm^{3+} ions doped borate phosphors have been reported by many researchers [9] but still the PL properties of Sm^{3+} ions doped alumino-borate phosphors need to be improved for the design and development of new luminescent devices.

In this paper, a novel intense tri-chromatic green/orange/red emitting phosphor, NABO:Sm^{3+} was synthesized and reported. Their photoluminescence properties under the near-UV excitation were evaluated in detail. Furthermore, critical distance of NABO:Sm^{3+} phosphors were discussed.

2. Experimental

2.1.Sample preparation

The powder samples NABO:Sm^{3+} were prepared by using solution combustion synthesis. In our previous work, many borate host materials were successfully synthesized using this method [10-16]. The stoichiometric amounts of high purity starting materials, $Na(NO_3)$ (A.R.), $Al(NO_3)_3.9H_2O$ (A.R.), (high purity 99.9%), $Sm(NO_3)_3.6H_2O$ (high purity 99.9%), H_3BO_3 (A.R.), $CO(NH_2)_2$ (A.R.) have been used for phosphors preparation. The stoichiometric amounts of the ingredients were thoroughly mixed in an Agate Mortar with adding little amount of double distilled water. The materials then transferred into China basin and heated on heating menthol at about 70°C so as to obtained clear solution. The solution was then introduced into a pre-heated muffle furnace maintained at temperature 550 °C for combustion. The solution boils; foams and ignites to burn with flame which gave a voluminous, foamy powder. Following the combustion, the resulting foamy samples were crushed to obtain fine particles and then annealed in a slightly reducing atmosphere provided by burning charcoal at temperature 750°C for 2 hr and suddenly cooled to room temperature.

2.2.Material Characterizations

The phase and surface morphology of as prepared phosphors were characterized by X-ray diffraction measurements using Rigaku Miniflex II X-ray Diffractometer with Cu Kα radiation (λ=1.54059 Å) with scan speed 2^0/min and Field emission - scanning electron microscopy (FE-SEM) (Hitachi, Model-S4800 type II). The PL & PLE measurements at room temperature were performed on Hitachi F-7000 Spectroflurometer with spectral resolution of 2.5 nm.

3. Results and Discussion

3.1. X-ray Diffraction Pattern

The XRD pattern of the host lattice of $Na_{2(0.97)}Al_2B_2O_7$: $_{0.03}Sm^{3+}$ is as shown in Fig. 1 and it was found to be in good agreement with the standard ICDD file No. 01-070-7606, the crystallographic data are given in Table 1. There are no observable differences between these diffraction patterns, indicating that a little amount of doped RE ions has almost no effect on the NABO crystalline structure. The ionic size of Sm^{3+} (0.958 Å) ion is smaller than that of Na^+ (1.02 Å) and Al^{3+} (0.54 Å) so the incorporation of the dopant may takes place in Na^+ lattice site in the crystal lattice.

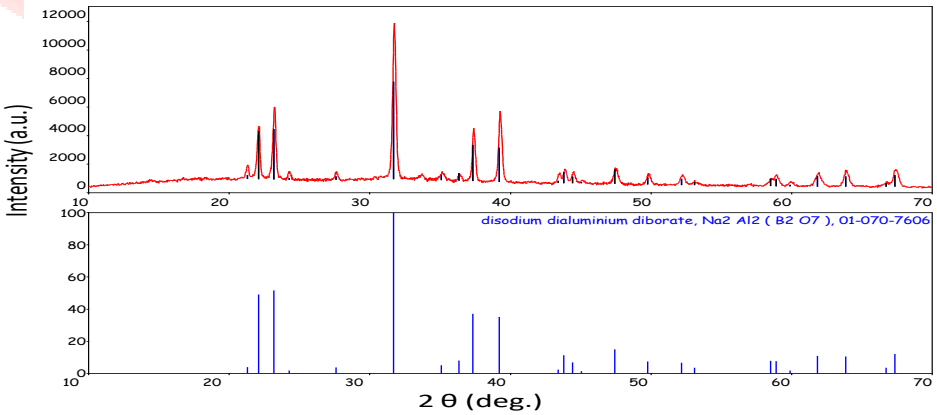

Fig 1. Powder XRD pattern of $Na_{2(0.97)}Al_2B_2O_7$: $_{0.03}Sm^{3+}$ phosphor.

Table 1. Crystallographic data of $Na_2Al_2B_2O_7$

Chemical Formula	$Na_2Al_2B_2O_7$
Crystal Structure	Hexagonal
Space Group	P-31c (163)
a (Å)	4.810
b (Å)	4.810
c (Å)	15.277
α (°)	90.00
β (°)	90.00
γ (°)	120.00
V (Å^3)	306.12
Z	2

3.2. FE-SEM micrographs of phosphor powders

The FE-SEM photographs of $Na_{2(0.97)}Al_2B_2O_7$: $_{0.03}Sm^{3+}$ powders prepared by solution combustion method is shown in Fig. 2. The shapes of the particles were observed to be random in nature with agglomeration for both the phosphors. The crystalline size of both the phosphors was observed to be varied in the range 0.3-2 µm.

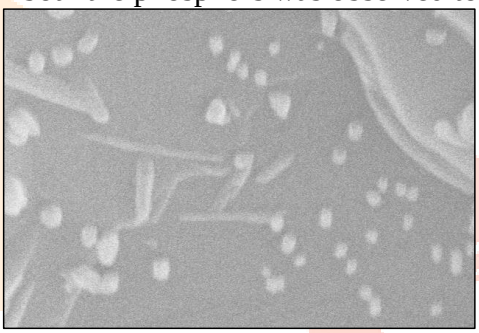

Fig 2. FE-SEM images of $Na_{2(0.97)}Al_2B_2O_7$: $_{0.03}Sm^{3+}$.

3.3. Photoluminescence Analysis

3.3.1. Photoluminescence properties of $Na_2Al_2B_2O_7$: Sm^{3+} phosphor

Fig. 3 depict the spectral characteristics of $Na_{2(0.97)}Al_2B_2O_7$: $_{0.03}Sm^{3+}$ phosphor. For 603 nm emission peak, the excitation spectra consist of several excitation peaks located at 305 ($^6H_{5/2}\rightarrow{}^4P_{5/2}$), 330($^6H_{5/2}\rightarrow{}^2L_{15/2}$), 344 ($^6H_{5/2}\rightarrow{}^4H_{9/2}$), 361 ($^6H_{5/2}\rightarrow{}^4D_{3/2}$), 374 ($^6H_{5/2}\rightarrow{}^4D$), 403 ($^6H_{5/2}\rightarrow{}^4F_{7/2}$), 462 ($^6H_{5/2}\rightarrow{}^4I_{13/2}$), and 473 nm ($^6H_{5/2}\rightarrow{}^4I_{11/2}$), which are attributed to the f–f forbidden transitions of Sm^{3+} ions, are observed within the wavelength region of 300 nm to 500 nm. It is noticed that the intensity of the f–f transition at 403 nm is higher than that of the other transitions. Thus, this transition is chosen for the measurement of the emission spectra of $Na_{2(1-x)}Al_2B_2O_7$: $_xSm^{3+}$ (x=0.005,0.01,0.02,0.03,0.04) phosphors. This finding also indicates that the as-prepared phosphor can be efficiently excited by NUV (~400 nm) LED chips. The emission spectra of $Na_{2(0.97)}Al_2B_2O_7$: $_{0.03}Sm^{3+}$ phosphor are shown in Fig. 4 (a). Four prominent groups of emission lines approximately ranging from 550 nm to700 nm can be attributed to the intra-4f orbital transition from the $^4G_{5/2}$ level to the ^6H_J (J = 5/2, 7/2, and 9/2) level because of their consistent luminescence behaviors with the Sm^{3+} emission characteristics [17-19]. Among these transitions, the first one at 565 nm ($^4G_{5/2}\rightarrow{}^6H_{5/2}$) is a magnetic-dipole (MD) transition, the second at 603 nm ($^4G_{5/2}\rightarrow{}^6H_{7/2}$) is a partly magnetic and partly forced electric-dipole (ED) transition, and the third at 651 nm ($^4G_{5/2}\rightarrow{}^6H_{9/2}$) is purely ED transition sensitive to the crystal field [20-21]. Notably, the $^4G_{5/2}\rightarrow{}^6H_{7/2}$ (603 nm) transition has the strongest intensity and can be applied to orange-red emitting display materials. Generally, the intensity ratio of ED and MD transitions can be used to understand the symmetry of the local environment of trivalent 4f ions in the host matrix [22]. The asymmetric nature is more prominent when the intensity of the ED transition is higher. The present study shows that the $^4G_{5/2}\rightarrow{}^6H_{9/2}$ transition (651 nm) of the Sm^{3+} ions has relatively lower emission intensity than the $^4G_{5/2}\rightarrow{}^6H_{5/2}$ transition (565 nm), which describes the symmetric nature of the host matrix investigated.

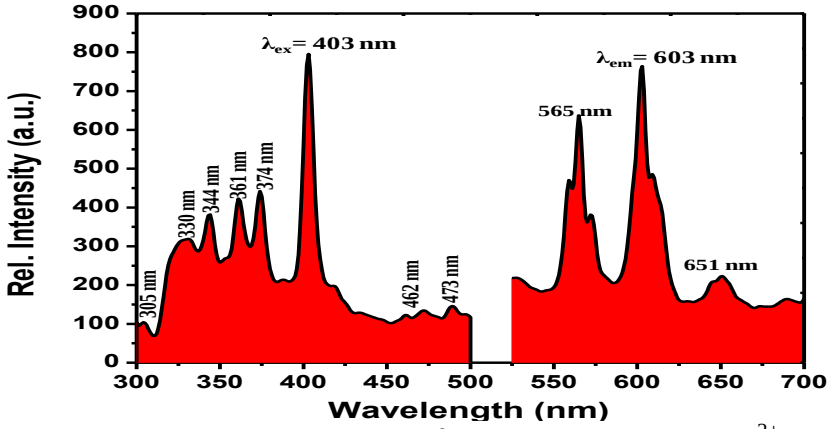

Fig 3. Excitation and emission spectra of $Na_{2(0.97)}Al_2B_2O_7$: $_{0.03}Sm^{3+}$ phosphor.

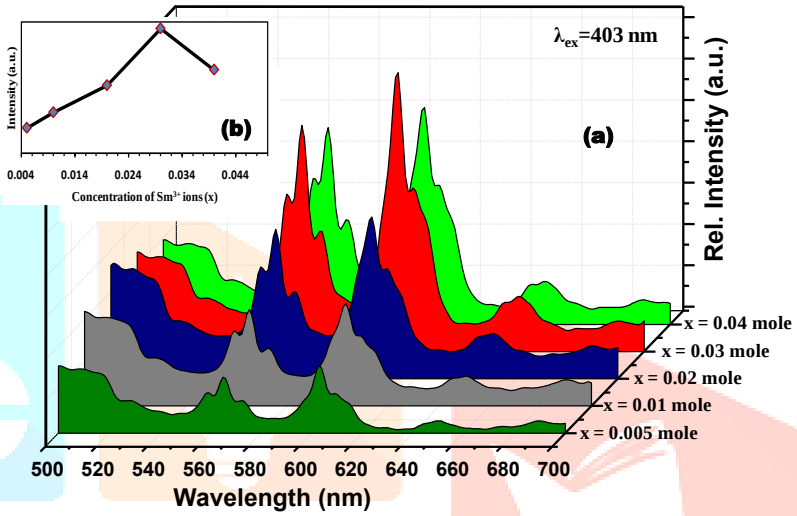

Fig 4. (a) Dependence of the PL intensities of $Na_{2(1-x)}Al_2B_2O_7$: $_xSm^{3+}$ at λ_{ex}=403 nm at different Sm^{3+} concentrations. (b) The top inset shows the influence of the concentration on the emission intensity of $Na_{2(1-x)}Al_2B_2O_7$: $_xSm^{3+}$ phosphor (x=0.005,0.01, 0.02, 0.03, and 0.04).

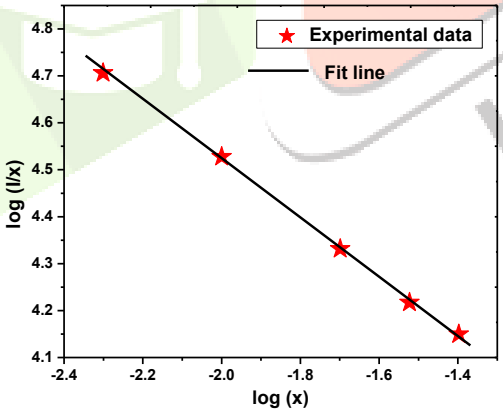

Fig 5. Plot of log(I/x) as function of log(x) in $Na_2Al_2B_2O_7$:Sm^{3+} phosphor (λ_{ex}=403 nm).

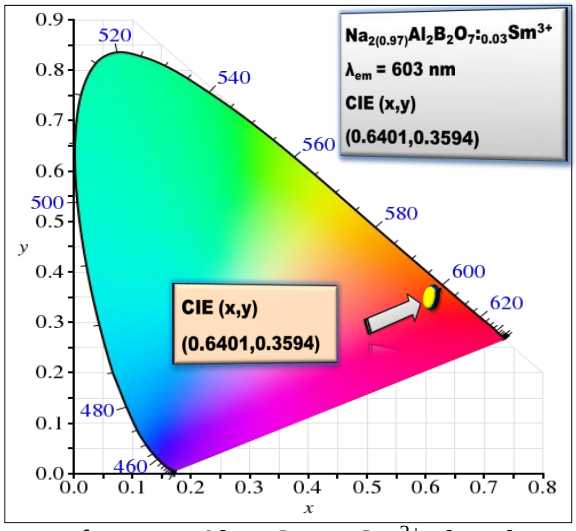

Fig 6. Chromaticity coordinates of $Na_{2(0.97)}Al_2B_2O_7$:$_{0.03}Sm^{3+}$ phosphor in the CIE 1931 chromaticity diagram.

3.3.2. Concentration quenching mechanism of $Na_2Al_2B_2O_7:Sm^{3+}$ phosphor

To study the effect of Sm^{3+} ion concentrations on the PL emission intensity of NABO:Sm^{3+} phosphor, a series of samples with different Sm^{3+} ion concentrations ranging from 0.5 mol% to 4 mol% were prepared. Fig. 4 (b) shows the variation in emission intensity with Sm^{3+} ion concentrations under 403 nm excitation. The emission intensity initially increases, reached the maximum at 3 mol% Sm^{3+}, and then decreases above 3 mol% with increased Sm^{3+} ion concentration. The decrease in PL emission intensity can be attributed to concentration quenching processes. The energy transfer from one activator to another generates the concentration quenching of luminescence. Blasse has pointed out that if the activator is introduced solely on Z ion sites, χc is the critical concentration, N is the number of Z ions in the unit cell and V is the volume of the unit cell, then there is on the average one activator ion per V/ χcN [23]. The critical transfer distance (Rc) is approximately equal to twice the radius of a sphere with this volume:

$$R_c \approx 2\left(\frac{3V}{4\pi\chi_c N}\right)^{1/3} \quad (1)$$

The critical transfer distance of the center Sm^{3+} in NABO phosphor by taking the appropriate values of V, N, and χc (535.62 Å, 6, and 0.03, respectively) is 18 Å. Generally, the resonant energy-transfer mechanism is governed by exchange and multipolar interactions. Previous studies have indicated that the critical distance between the sensitizer and the activator should be shorter than 3 Å to 4 Å when the energy transfer results from exchange interaction [24], which is far less than that of the above calculation result of Sm^{3+} doped NABO. This finding suggests that the energy transfer among Sm^{3+} ions in NABO:Sm^{3+} phosphor does not occur in this case. Therefore, the process of energy transfer should be electric multipole interaction. The emission intensity (I) per activator ion follows the equation:

$$\frac{I}{x} = K[1 + \beta(x)^{Q/3}]^{-1} \quad (2)$$

where χ is the activator concentration; Q is a constant of multipolar interaction and equals 6, 8, or 10 for dipole–dipole; dipole–quadrupole or quadrupole–quadrupole interaction, respectively; and K and β are constants under the same excitation condition for the given host crystal. The curve of log(I/x) vs. log(x) in NABO:Sm^{3+} phosphor is shown in Fig. 5. The figure clearly shows that the relation between log(I/x) and log(x) is approximately linear and the slope is about -1.824. The Q value calculated based on the linear fitting using Eq. (2) is 5.472, which is close to 6. This finding indicates that the dipole–dipole interaction is the major mechanism for the concentration quenching of the fluorescence emission of Sm^{3+} ions in NABO phosphor. The CIE chromaticity coordinates for $Na_{2(0.97)}Al_2B_2O_7$:$_{0.03}Sm^{3+}$ were calculated from the PL spectra under 403 nm excitation and marked with a white circular symbol in the CIE 1931 chromaticity diagram in Fig. 6. The chromaticity coordinates (x,y) of this phosphor are calculated to be (0.64, 0.35), respectively, which indicates that the emission color of the as prepared phosphors is located in the reddish-orange region.

Conclusions

Rare earth Sm^{3+} activated NABO phosphors were successfully synthesized by using solution combustion technique. The XRD patterns confirmed their tetragonal structure and the FE-SEM images showed the closely packed particles with agglomerate phenomenon. Based on the theoretical calculations, it is found that the electric multipolar interaction is the major mechanism for concentration quenching of NABO:Sm^{3+} phosphor and the critical transfer distance was found to be 21.51 Å. The PL emission spectra of Sm^{3+} ions gives emission spectrum with a maximum intensity at 601 nm under 403 nm excitation which may be useful for solid state lighting applications.

Acknowledgments

One of the authors Ritesh S. Palaspagar is thankful to the Chairman of FIST-DST project SGB Amravati University Amravati, for providing XRD facility to this work.

References

[1] Peters T. E., Baglio J., 1970, Luminescence and structural properties of alkaline earth chloroborates activated with divalent europium, J. Inorg Nucl Chem. 32(4), 1089.
[2] Jyothi L., Upender G., Kuladeep R., Rao D. N., 2014, Structural, thermal, optical properties and simulation of white light of titanium-tungstate-tellurite glasses doped with dysprosium, Mater. Res. Bull., 50, 424.
[3] Othman H. A., Elkholy H. S., Hager I. Z., 2017, Structural and optical investigation of undoped and Sm^{3+} doped lead oxyfluoroborate glasses, Mater. Res. Bull., 89, 210.
[4] Ramachari D., Moorthy L. R., Jayasankar C. K.,2013, Spectral investigations of Sm^{3+} doped oxyfluorosilicate glasses, Mater. Res. Bull., 48(9), 3607.
[5] Hussain N. S., Aruna V., Buddhudu S., 2000, Absorption and photoluminescence spectra of Sm^{3+}:TeO_2–B_2O_3–P_2O_5–Li_2O glass, Mater. Res. Bull., 35(5), 703.
[6] Deopa N., Rao A. S., Gupta M., Vijaya Prakash G., 2018, Spectroscopic investigations of Nd^{3+} doped Lithium Lead Alumino Borate glasses for 1.06 μm laser applications, Opt. Mater., 75, 127.
[7] Mahamuda S. K., Swapna K., Packiyaraj P., Rao A. S., Vijaya Prakash G., 2014, Lasing potentialities and white light generation capabilities of Dy^{3+} doped oxy-fluoroborate glasses, J. Lumin., 153, 382.
[8] Arunkumar S., Marimuthu K., 2013, Concentration effect of Sm^{3+} ions in B_2O_3–PbO–PbF_2–Bi_2O_3–ZnO glasses – Structural and luminescence investigations, J. Alloys Compd., 565, 104.
[9] Bedyal A. K., Vinay Kumar, Ntwaeaborwa O. M, Swart H. C., 2014, A promising orange-red emitting nanocrystalline $NaCaBO_3$:Sm^{3+} phosphor for solid state lightning, mat. res. exp., 1(1), 015006.
[10] Palaspagar R. S., Gawande A. B., Sonekar R. P., Omanwar S. K., 2014, Combustion synthesis and photoluminescence properties of a novel Eu^{3+} doped lithium alumino-borate phosphor, J. Lumin., 154, 58.
[11] Palaspagar R. S., Gawande A. B., Sonekar R. P., Omanwar S. K., 2015, Fluorescence properties of Tb^{3+} and Sm^{3+} activated novel $LiAl_7B_4O_{17}$ host via solution combustion synthesis, Mater. Res. Bull., 72, 215.
[12] Palaspagar R. S., Sonekar R. P., Omanwar S. K., 2013, Novel inorganic borate host phosphor $K_2Al_2B_2O_7$:Dy^{3+} for LED based solid state lighting, AIP Conference Proceedings, 1536(1), 807.
[13] Palaspagar R. S., Sonekar R. P., Omanwar S. K., 2015, Synthesis and luminescent properties of Tb^{3+} activated novel magnesium alumino-borate phosphor, J. Chin. Adv. Mater. Soc., 3(3), 170.
[14] Palaspagar R. S., Sonekar R. P., Omanwar S. K., 2016, Fluorescence properties and energy transfer investigation of novel $Li_2Al_2B_2O_7$:Ce^{3+}, Tb^{3+} phosphors via combustion synthesis, J. Mater. Sci. Mater. Electron., 27(5), 4951.
[15] Palaspagar R. S., Gawande A. B., Sonekar R. P., Omanwar S. K., 2015, $Eu^{3+} \rightarrow Eu^{2+}$ reduction in $BaAl_2B_2O_7$ phosphor in oxidizing environment, Opt. Int. J. Light Electron opt., 126(24), 5030.
[16] Palaspagar R. S., Sonekar R. P., Omanwar S. K., 2016, NUV excited luminescence of Eu^{3+} doped inorganic $NaCa_{0.5}Al_2B_2O_7$ phosphor via slow evaporation technique, J. Mater. Sci. Mater. Electron., 27(9), 9335.
[17] Sheng T., Fu Z., Wang X., Zhou S., Zhang S., Dai Z., 2012, Solvothermal Synthesis and Luminescence Properties of $BaCeF_5$, and $BaCeF_5$: Tb^{3+}, Sm^{3+} Nanocrystals: An Approach for White Light Emission, J. Phys. Chem. C., 116(36), 19597.
[18] Zhang J., Hu R., Qin Q., Wang D., Liu B., Wen Y., Zhou M., Wang Y., 2012, The origin of two quenching concentrations and unusual afterglow behaviors of Ba_2SnO_4:Sm^{3+} phosphor, J. Lumin., 132(10), 2590.
[19] Park S., 2012, Luminescent properties of $Sr_{2.5-3x/2}Ba_{0.5}Sm_xAlO_4F$ oxyfluorides, J. Lumin., 132(4), 875.
[20] Raju G. S. R., Buddhudu S., 2008, Emission analysis of Sm^{3+} and Dy^{3+}: $MgLaLiSi_2O_7$ powder phosphors, Spectrochim. Acta, Part A., 70(3), 601.
[21] Singh V., Watanabe S., Rao T. K. G., Chubaci J. F. D., Kwak H. Y., 2010, Luminescence and defect centres in $MgSrAl_{10}O_{17}$:Sm^{3+} phosphor, J. Non-cryst. Solids., 356(23), 1185.
[22] Xia Z., Chen D., 2010, Synthesis and Luminescence Properties of $BaMoO_4$:Sm^{3+} Phosphors, J. Am. Ceram. Soc., 93(5), 1397.
[23] Blasse G., Grabmaier B.C., 1994, Energy Transfer, Springer Verlag, Berlin, 91.
[24] Antipeuko B.M., Bataev I. M., Ermolaev V. L., Lyubimov E. I., Privalova T. A., 1970, Radiationless transfer of electron excitation energy between rare earth ions in $POCl_3$-$SnCl_4$, Opt. Spectrosc., 29(2), 335.